

EFFECT OF Ce^{3+} METAL IONS ON THE ANTIBACTERIAL AND ANTICANCER ACTIVITY OF ZINC OXIDE NANOPARTICLES PREPARED BY COPRECIPITATION METHOD

THEIVARASU C¹, INDUMATHI T²

¹Department of Chemistry, PSG College of Technology, Coimbatore, Tamil Nadu. ²Department of Science and Humanities, Science and Humanities, Sri Krishna College of Engineering and Technology, Coimbatore, Tamil Nadu. Email: theiva_psg@yahoo.co.in

Received: 26 November 2016, Revised and Accepted: 15 December 2016

ABSTRACT

Objective: This study was undertaken to know about the antibacterial and anticancer activity of synthesized zinc oxide (ZnO) nanoparticles (NPs).

Methods: The ZnO NPs and different concentration of Ce^{3+} (0.05M, 0.10M, and 0.15M)-doped ZnO NPs were synthesized by coprecipitation method. The synthesized nanoparticles were analyzed by X-ray diffraction (XRD) and HRSEM. The antibacterial studies were performed against a set of bacterial strains as Gram-positive bacteria (*Streptococcus aureus* and *Streptococcus pneumoniae*) and Gram-negative (*Escherichia coli*, *Pseudomonas aeruginosa*, *Proteus vulgaris*, *Klebsiella pneumoniae*, and *Shigella dysenteriae*) bacteria. The cytotoxic effect of ZnO and Ce-doped ZnO was analyzed in cultured (A549) human lung cancer cell line.

Result: The XRD studies showed the wurtzite structure of nanoparticles. HRSEM analysis showed the spherical shape of ZnO and Ce-doped ZnO. The $Zn_{0.85}Ce_{0.15}O$ NPs possessed more antibacterial effect as compared to the other ZnO and Ce-doped ZnO NPs. The $Zn_{0.90}Ce_{0.10}O$ NPs created the highest cytotoxicity activity. With respect to cell death, as low a concentration of 68 ± 0.05 $\mu\text{g/ml}$ of $Zn_{0.90}Ce_{0.10}O$ NPs was good enough to cause loss of viability of 50% of the cell as compared to ZnO and $Zn_{1-x}Ce_xO$ ($x=0.05$ and 0.15) NPs.

Conclusion: Results from this work concluded that $Zn_{0.85}Ce_{0.15}O$ and $Zn_{0.90}Ce_{0.10}O$ NPs possess antibacterial and anticancer activity, respectively.

Keywords: Zinc oxide nanoparticles, Coprecipitation method, Antibacterial activity and anticancer activity, Human lung cancer cell line.

© 2017 The Authors. Published by Innovare Academic Sciences Pvt Ltd. This is an open access article under the CC BY license (<http://creativecommons.org/licenses/by/4.0/>) DOI: <http://dx.doi.org/10.22159/ajpcr.2017.v10i3.16350>

INTRODUCTION

Zinc oxide nanoparticles (ZnONPs) are well recognized as a biocompatible multifunctional material with exceptional semiconducting, optical, and piezoelectric properties [1]. These materials are used in different potential application such as light-emitting diodes, lasers, sensors, actuators, transducers, and nanogenerators [1-6]. ZnO is one of the important semiconductor materials for wide band gap 3.36 eV and large exciton binding energy 60 meV at room temperature. This makes us interesting for its electro-optical applications [7].

The metal oxide nanomaterials are attractive for use in biomedical applications. It has been proposed that the high surface area of metal oxide nanoparticles significantly enhances their ability to produce reactive oxygen species (ROS) [8,9]. Toxicity of ZnO NPs is reported due to the generation of intracellular ROS and dissolved Zn ions [10]. ROS is generated through various mechanisms such as illumination of nanomaterials by ultraviolet (UV) light, disturbance of intracellular metabolic activities, and antioxidant system, result in the generation of oxidative stress in the cells. ROS can damage DNA, cell membrane, and proteins which may lead to cell death [11,12].

To traverse new strategies to discuss and develop the next generation of drugs or agents to control bacterial infections and cytotoxic effects, the antibacterial and anticancer properties of ZnO and Ce-doped ZnO NPs are examined with the support of the structural and optical characterization studies.

METHODS

Synthesis

Zinc (II) nitrate hexahydrate (AR), cerium (III) nitrate hexahydrate (AR), and NaOH (AR) are used as precursor without further purification. The

details of experimental procedure for the preparation of pure ZnO and $Zn_{1-x}Ce_xO$ ($x=0.05$, 0.10 M, and 0.15 M) samples have been reported in our previous paper [7].

Antibacterial activity

The antibacterial activity of ZnO and Ce-doped ZnO NPs was investigated by disc diffusion method against the test Gram-positive bacteria (*Streptococcus aureus* and *Streptococcus pneumoniae*) and Gram-negative bacteria (*Escherichia coli*, *Pseudomonas aeruginosa*, *Proteus vulgaris*, *Klebsiella pneumoniae*, and *Shigella dysenteriae*) on Mueller-Hinton agar (MHA), according to the Clinical and Laboratory Standards Institute [13]. The media plates (MHA) were streaked with bacteria 2-3 times by rotating the plate at 60° angles for each streak to ensure the homogeneous distribution of the inoculums. After inoculation, discs (6 mm Hi-Media) loaded with 1mg of the test samples were placed on the bacteria-seeded disc plates using sterile forceps. The plates were then incubated at 37°C for a day. The inhibition zone around the disc was measured and recorded. Amoxicillin (Hi-Media) was used as the positive controls against Gram-positive bacteria and Gram-negative bacteria, respectively, to compare the efficacy of the test samples.

Cell culture

The A549 human lung cancer cell line was obtained from the National Center for Cell Science, Pune, India. The cells were cultured in DMEM high glucose medium (Sigma-Aldrich, USA), supplemented with 10% fetal bovine serum (Gibco), and 20 ml of penicillin/streptomycin as antibiotics (Gibco), in 96-well culture plates, at 37°C in a humidified atmosphere of 5% CO_2 in a CO_2 incubator (Thermo Scientific, USA). All experiments were performed using cells from passage 15 or less.

Cell viability assay

The ZnO and Ce-doped ZnO NPs were suspended in dimethyl sulfoxide (DMSO) to make stock solution. These stock solutions were

diluted separately with media to get various concentrations of the complex. Two hundred milliliters of these samples was added to wells containing 5×10^3 A549 cells per well. DMSO solution was used as the solvent control. After 24 hr, 20 μ l of 3-(4, 5-di-methylthiazol-2-yl)-2, 5-diphenyl-2H-tetrazolium bromide solution (5 mg/ml in phosphate-buffered saline [PBS]) was added to each well, and the plate was covered with aluminum foil and incubated for 4 hr at 37°C [14]. The purple formazan outcome was disposed by adding 100 μ l of DMSO to each well. The absorbance was recorded at 570 nm (measurement) and 630 nm (reference) using a 96-well plate reader (Bio-Rad, iMark, USA). Data were possessed for three replicates each and were used to calculate the respective mean. The percentage inhibition was calculated from the data using the formula:

$$\text{Mean OD of untreated cells (control)} \\ = \frac{\text{Mean OD of untreated cells (control)} - \text{Mean OD of treated cells}}{\text{Mean OD of untreated cells (control)}} \times (100)$$

Acridine orange (AO) and ethidium bromide (EB) staining

Apoptotic morphology was investigated by AO/EB double-staining method as described by Spector *et al.* with some modifications [15]. Briefly, the cells are treated with IC_{50} concentration of ZnO and Ce-doped ZnO for a day. After incubation, the cells were harvested and washed with cold PBS. Cell pellets were diluted with PBS to a concentration of 5×10^5 cells/ml and mixed with 25 μ l of AO/EB solution (3.8 μ M of AO and 2.5 μ M of EB in PBS) on clean microscope slide and immediately examined under fluorescent microscope (Carl Zeiss, Axioscope2plus) with UV filter (450-490 nm).

The X-ray diffraction (XRD) patterns were recorded using (PANalytical X'Pert Pro). The surface morphology was studied through FEI QUANTA 250 scanning electron microscope (SEM).

RESULTS AND DISCUSSION

XRD studies

From Fig. 1, the XRD pattern confirmed the synthesis of ZnO and Ce-doped ZnO NPs is in hexagonal wurtzite structure. The Ce-doped ZnO NPs have no impurity peaks and are detected as Ce^{3+}/Ce^{4+} ions with cerium oxide between CeO_2 and Ce_2O_3 . The lattice constant "a" and "c" values at 3.2521 Å and 5.2111 Å for pure ZnO NPs. The substitution of Ce^{3+} ion instead of Zn^{2+} ion at their lattice site increases. The changes in lattice parameter values are due to the broadness of ZnO lattice by the substitution of Ce^{3+} (1.02 Å) ion to Zn^{2+} (0.74 Å) sites, with a greater ionic radius compared to Zn^{2+} in their tetrahedral coordinates. The lattice constant "a" and "c" values are (3.2540 Å, 3.2539 Å, and 3.2543 Å) and (5.2138 Å, 5.2150 Å, and 5.2113 Å) for $Zn_{0.95}Ce_{0.05}O$, $Zn_{0.90}Ce_{0.10}O$, and $Zn_{0.85}Ce_{0.15}O$ NPs, respectively. The average crystalline size was 39, 32, 30, and 27 nm for ZnO and Ce-doped ZnO NPs, respectively. The decrease in D is mainly because of the distortion in the host ZnO lattice by the foreign impurity, i.e., Ce^{3+} [7].

Field emission SEM analysis

Fig. 2 shows the HRSEM image of ZnO and Ce-doped ZnO NPs. The unadulterated ZnO NPs and Ce-doped ZnO NPs are found to be in spherical-shaped morphology. Different concentration of Ce-doped ZnO NPs agglomerates with each other due to the increasing nucleation of Ce^{3+} ions and subsequent growth of ZnO NPs [7].

Antibacterial activity

Antibacterial activity of (Zn) ZnO and Ce-doped ZnO as Ce1, Ce2, and Ce3 is investigated against Gram-positive bacteria (*S. aureus* and *S. pneumonia*) and Gram-negative bacteria (*E. coli*, *P. aeruginosa*, *P. vulgaris*, *K. pneumonia*, and *S. dysenteriae*) are studied by disc diffusion method as shown in Fig. 3. Fig. 4 communicates the area of zone inhibition, and the activity as antibacterial which surrounds each ZnO and Ce-doped ZnO NPs filled with test specimen.

The antibacterial efficacy of ZnO NPs is commonly influenced by ROS, which is mainly related to the size, larger surface area, an increase in

oxygen vacancies, the diffusion capacity of the reactant, and the release of Zn^{2+} [16].

From antibacterial activity, ZnO and Ce-doped ZnO NPs; $Zn_{0.85}Ce_{0.15}O$ NPs possessed more antibacterial effect as compared to the other ZnO, $Zn_{0.95}Ce_{0.05}O$, and $Zn_{0.90}Ce_{0.10}O$ NPs. Increasing the concentration of Ce^{3+} increases the zone of inhibition.

The smaller sized NPs indeed have higher activity as antibacterial [17,18]. The XRD pattern shows the particles size of ZnO and Ce-doped ZnO NPs as 39, 32, 30, and 27 nm, respectively. $Zn_{0.85}Ce_{0.15}O$ NPs particles' size is lesser as compared to the other ZnO, $Zn_{0.95}Ce_{0.05}O$, and $Zn_{0.90}Ce_{0.10}O$

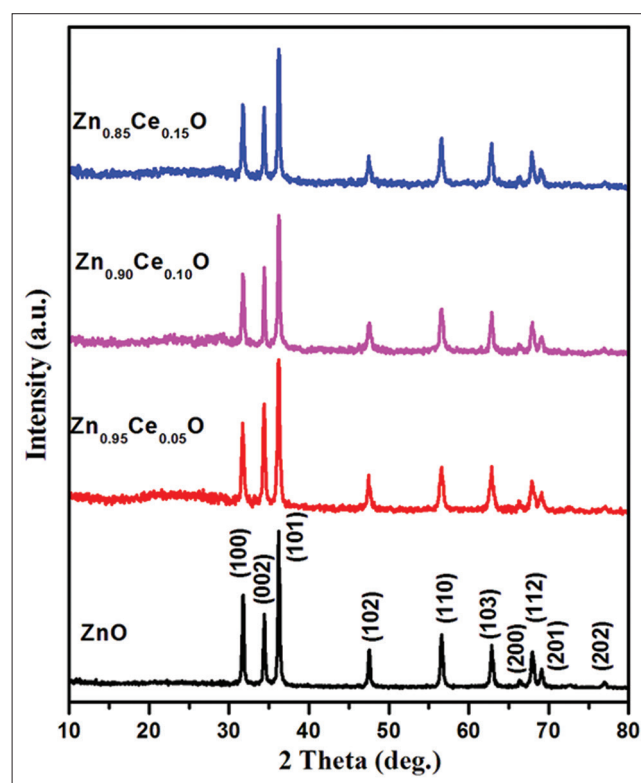


Fig. 1: X-ray diffraction pattern of the pure zinc oxide, $Zn_{0.95}Ce_{0.05}O$, $Zn_{0.90}Ce_{0.10}O$, and $Zn_{0.85}Ce_{0.15}O$ nanoparticles [7]

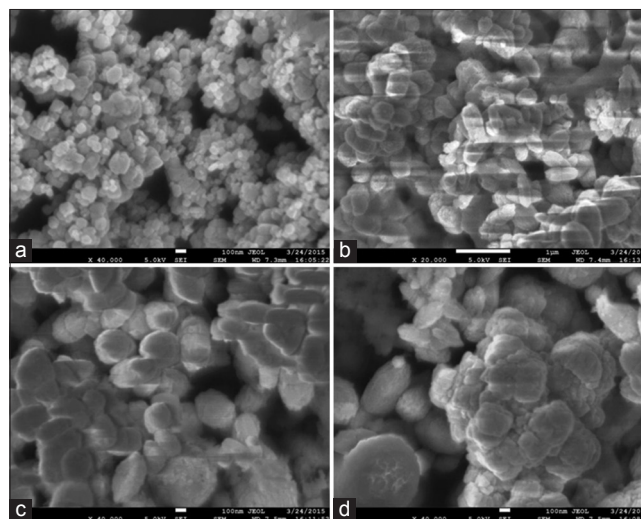


Fig. 2: HRSEM images of the (a) zinc oxide, (b) $Zn_{0.95}Ce_{0.05}O$, (c) $Zn_{0.90}Ce_{0.10}O$, and (d) $Zn_{0.85}Ce_{0.15}O$ nanoparticles [7]

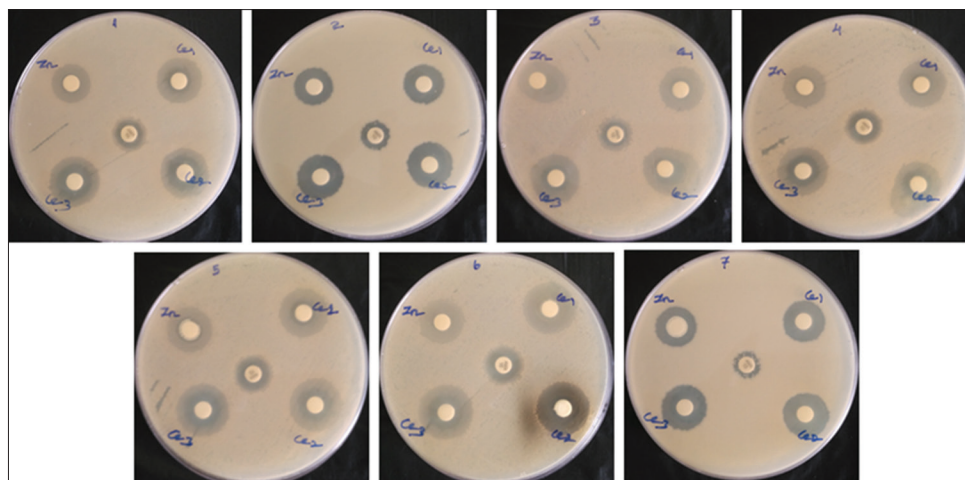


Fig. 3: The antibacterial activity of the zinc oxide and $Zn_{1-x}Ce_xO$ ($x=0.05, 0.10, \text{ and } 0.15$) against Gram-positive (*Streptococcus aureus* (2) and *Streptococcus pneumoniae* (6)) and Gram-negative (*Escherichia coli* (4), *Pseudomonas aeruginosa* (5), *Proteus vulgaris* (7), *Klebsiella pneumoniae* (1), and *Shigella dysenteriae* (3))

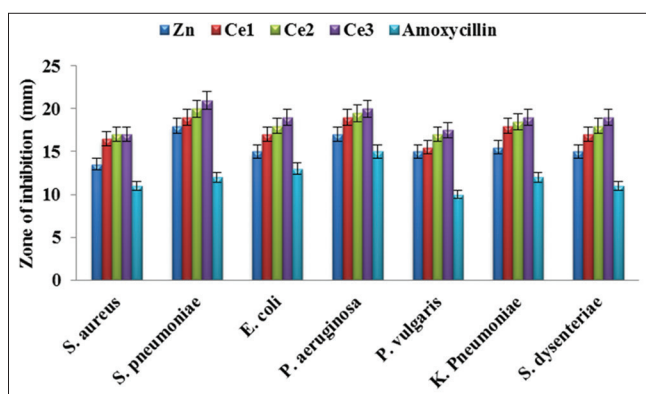


Fig. 4: The size of the zone inhibition surrounding each disc, filled with test samples specifies the activity as antibacteria toward Gram-positive (*Streptococcus aureus* and *Streptococcus pneumoniae*) and Gram-negative (*Escherichia coli*, *Pseudomonas aeruginosa*, *Proteus vulgaris*, *Klebsiella pneumoniae*, and *Shigella dysenteriae*) for the zinc oxide and $Zn_{1-x}Ce_xO$ ($x=0.05, 0.10, \text{ and } 0.15$) nanoparticles

NPs [7]. The particle with a small size can easily penetrate into bacterial membranes due to their large interfacial area, thus enhancing their antibacterial efficiency.

From the photoluminescence spectra, wavelengths of the blue emissions values are at 440, 439, 439, and 446 nm for ZnO and Ce-doped ZnO NPs. This illustrates the larger count defects such as zinc and oxygen vacancies in the $Zn_{0.85}Ce_{0.15}O$ NPs. Thus, there are increased count of ROS as compared to ZnO and $Zn_{1-x}Ce_xO$ ($x=0.05$ and 0.10) NPs.

Anticancer properties

The cytotoxic effect of the ZnO and $Zn_{1-x}Ce_xO$ ($x=0.05, 0.10, \text{ and } 0.15$) NPs were examined in cultured (A549) human lung cancer cell line by exposing cells for 24 hr to culture medium containing unmixed ZnO, $Zn_{0.95}Ce_{0.05}O$, $Zn_{0.90}Ce_{0.10}O$, and $Zn_{0.85}Ce_{0.15}O$ NPs at 280 ± 0.05 , 82 ± 0.05 , 68 ± 0.05 , and 76 ± 0.05 $\mu\text{g/ml}$ for IC_{50} concentration as shown in Fig. 5a-d. In relation to cell death, a minimum concentration 68 ± 0.05 $\mu\text{g/ml}$ for 24 hr treatment of $Zn_{0.90}Ce_{0.10}O$ NPs was well enough to induce 50% cell mortality as compared to other ZnO, $Zn_{0.95}Ce_{0.05}O$, and $Zn_{0.85}Ce_{0.15}O$ NPs. The $Zn_{0.90}Ce_{0.10}O$ NPs showed a highly effective cytotoxic activity against (A549) human lung cancer

cell. The cytotoxic efficiency of the ZnO NPs generally depends on the presence of ROS.

AO and EB staining

The most important characteristics of apoptosis are morphological changes during cell death. Fig. 6 represents that AO/EB double-stained A549 human lung cancer cell line treated with test substances 24 hr underwent both early apoptosis and late apoptosis. The control or viable cells show green fluorescence and normal cell features of uniform chromatin with an intact cell membrane, whereas the early apoptosis cells showed bright green region with yellowish green nuclear fragmentation and membrane bubbles and apoptotic bodies outside. The late apoptosis cells exhibited orange-yellow or red nuclei with condensed or fragmented chromatin. The results demonstrate that all substances induce the majority of cell death through apoptosis mode and very fewer in necrosis for 24 hr treatment. Chromatin condensation and fragmentation were observed in ZnO and $Zn_{1-x}Ce_xO$ ($x=0.05, 0.10, \text{ and } 0.15$) NPs treated cells.

The cellular toxicity mechanisms are based on ROS production, which exceeds the capacity of cellular antioxidant defense system causes cells to enter the state of oxidative stress. These oxidative stresses damage the cellular components such as lipids, proteins, and DNA [19,20]. The oxidation of fatty acids leads to the generation of lipid peroxides that initiates a chain reaction leading to disruption of plasma, organelle membranes, and subsequent cell death by induction of apoptosis. The ROS act as the critical signaling mechanism in the induction of apoptosis/cell death by many different stimuli [21,22].

CONCLUSIONS

Thus ZnO and Ce-doped ZnO NPs were prepared by co-precipitation method. From the XRD pattern, ZnO and Ce-doped ZnO NPs were revealed as wurtzite structure. The average crystallite sizes were calculated as 39, 32, 30, and 27 nm for ZnO and Ce-doped ZnO NPs, respectively. HRSEM image showed the spherical shape of ZnO and Ce-doped ZnO NPs. From antibacterial result, $Zn_{0.85}Ce_{0.15}O$ NPs possessed more antibacterial effect as compared to the other ZnO and $Zn_{1-x}Ce_xO$ ($x=0.05$ and 0.10) NPs. The cytotoxic effect of the ZnO and $Zn_{1-x}Ce_xO$ ($x=0.05, 0.10, \text{ and } 0.15$) NPs were examined in cultured (A549) human lung cancer cell line, in which the $Zn_{0.90}Ce_{0.10}O$ NPs showed the highest cytotoxic activity. With reference to cell death, a minimum concentration of 68 ± 0.05 $\mu\text{g/ml}$ of the $Zn_{0.90}Ce_{0.10}O$ NPs was well enough to induce 50% cell mortality as compared to ZnO and $Zn_{1-x}Ce_xO$ ($x=0.05$ and 0.15) NPs, respectively.

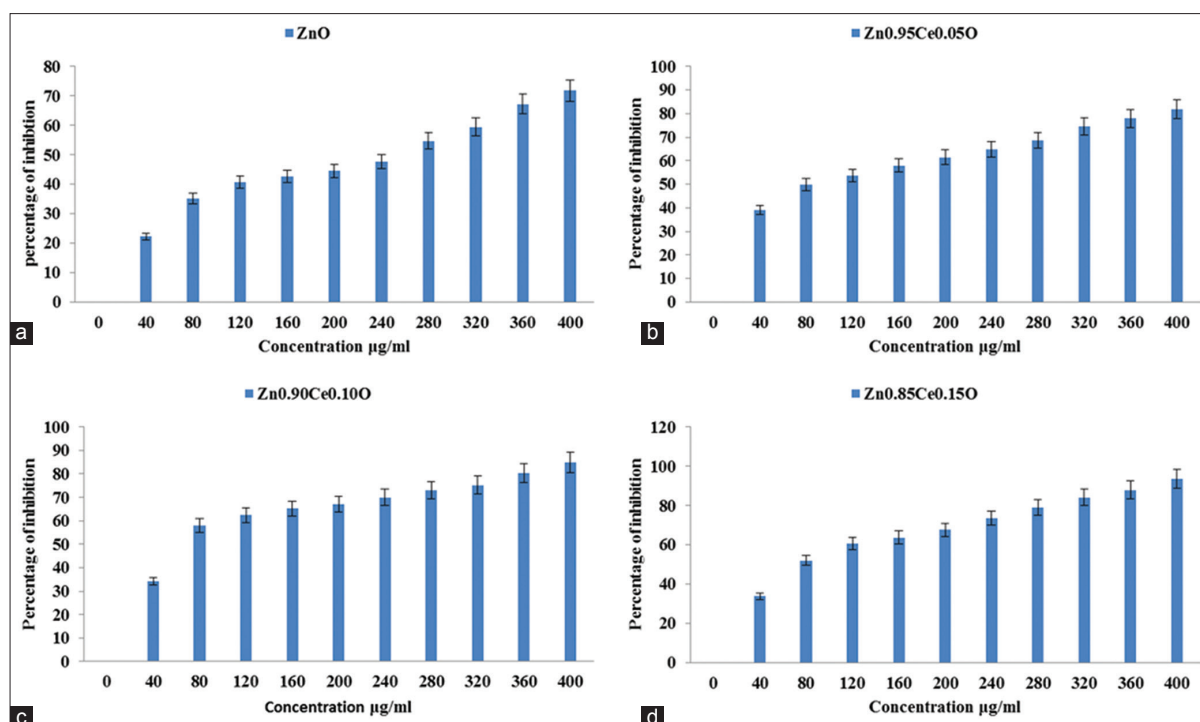


Fig. 5: (a) The effect of zinc oxide nanoparticles (NPs) on the cytotoxicity property in human lung cancer cell line (A549). (b) The effect of Zn_{0.95}Ce_{0.05}O NPs on the cytotoxicity property in human lung cancer cell line (A549). (c) The effect of Zn_{0.90}Ce_{0.10}O NPs on the cytotoxicity property in human lung cancer cell line (A549). (d) The effect of Zn_{0.85}Ce_{0.15}O NPs on the cytotoxicity property in human lung cancer cell line (A549)

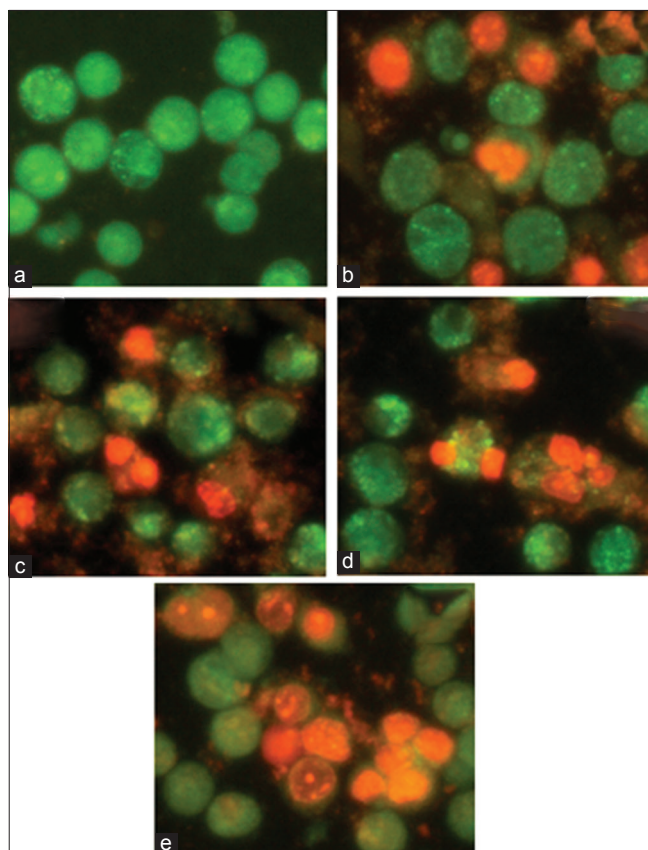


Fig. 6: Cells treated with (a) control (b) zinc oxide, (c) Zn_{0.95}Ce_{0.05}O, (d) Zn_{0.90}Ce_{0.10}O, and (e) Zn_{0.85}Ce_{0.15}O nanoparticles at the respective IC₅₀ concentrations and the morphologies observed after staining with acridine orange/ethidium bromide

REFERENCES

1. Wang ZL. Splendid one-dimensional nanostructures of zinc oxide: A new nanomaterial family for nanotechnology. *ACS Nano* 2008;2(10):1987-92.
2. Fan Z, Lu JG. Zinc oxide nanostructures: Synthesis and properties. *J Nanosci Nanotechnol* 2008;5(1):1561-73.
3. Huang MH, Wu Y, Feick H, Tran N, Weber E, Yang P. Catalytic growth of zinc oxide nanowires by vapor transport. *Adv Mater* 2001;13(2):113-6.
4. Wang X, Liu J, Song J, Wang ZL. Integrated nanogenerators in biofluid. *Nano Lett* 2007;7(8):2475-9.
5. Lao CS, Park MC, Kuang Q, Deng Y, Sood AK, Polla DL, *et al.* Giant enhancement in UV response of ZnO nanobelts by polymer surface-functionalization. *J Am Chem Soc* 2007;129(40):12096-7.
6. Wang X, Song J, Summers CJ, Ryou JH, Li P, Dupuis RD, *et al.* Density-controlled growth of aligned ZnO nanowires sharing a common contact: A simple, low-cost, and mask-free technique for large-scale applications. *J Phys Chem B* 2006;110(15):7720-4.
7. Theivarasu C, Indumathi T. Effect of rare earth metal ion Ce³⁺ on the structural, optical and magnetic properties of ZnO nanoparticles synthesized by the co-precipitation method. *J Mater Sci Mater Electron* 2016;27:1-8.
8. Møller P, Jacobsen NR, Folkmann JK, Danielsen PH, Mikkelsen L, Hemmingsen JG, *et al.* Role of oxidative damage in toxicity of particulates. *Free Radic Res* 2010;44(1):1-46.
9. Li N, Sioutas C, Cho A, Schmitz D, Misra C, Sempf J, *et al.* Ultrafine particulate pollutants induce oxidative stress and mitochondrial damage. *Environ Health Perspect* 2003;111(4):455-60.
10. Sasidharan A, Chandran P, Menon D, Raman S, Nair S, Koyakutty M. Rapid dissolution of ZnO nanocrystals in acidic cancer microenvironment leading to preferential apoptosis. *Nanoscale* 2011;3(9):3657-69.
11. Desnues B, Cuny C, Grégori G, Dukan S, Aguilaniu H, Nyström T. Differential oxidative damage and expression of stress defence regulons in culturable and non-culturable *Escherichia coli* cells. *EMBO Rep* 2003;4(4):400-4.
12. Aertsen A, Michiels CW. Stress and how bacteria cope with death and survival. *Crit Rev Microbiol* 2004;30(4):263-73.
13. Vedernikova I. Synthesis and evaluation of Zinc substituted magnetite nanoparticles for drug delivery systems. *Int J Pharm Pharm Sci* 2015;7(9):177-80.

14. Amruthraj NJ, Preetamraj JP, Saravanan S, Lebel LA. *In vitro* studies on anticancer activity of capsaicinoids from capsicum Chinese against human hepatocellular carcinoma cells. *Int J Pharm Pharm Sci* 2014;6(4):254-8.
15. Spector DL, Goldman RD, Leinwand LA. *Cell: A Laboratory Manual*. Cold Spring Harbor, NY: Cold Spring Harbor Laboratory Press; 1998. p. 34.1-9.
16. Becker J, Raghupathi KR, Pierre JS, Zhao D, Koodali RT. Tuning of the crystallite and particle sizes of ZnO nanocrystalline materials in solvothermal synthesis and their photocatalytic activity for dye degradation. *J Phys Chem C* 2011;115(28):13844-50.
17. Zhang L, Ding Y, Povey M, York D. ZnO nanofluids – A potential antibacterial agent. *Prog Nat Sci* 2008;18:939-44.
18. Wilson A, Prabukumar S, Sathishkumar G, Sivaramakrishnan S. *Aspergillus flavus* mediated silver nanoparticles synthesis and evaluation of its antimicrobial activity against different human pathogens. *Int J Appl Pharm* 2016;8(4):43-6.
19. Lovric J, Bazzi HS, Cuie Y, Fortin GR, Winnik FM, Maysinger D. Differences in subcellular distribution and toxicity of green and red emitting CdTe quantum dots. *J Mol Med (Berl)* 2005;83(5):377-85.
20. Long TC, Saleh N, Tilton RD, Lowry GV, Veronesi B. Titanium dioxide (P25) produces reactive oxygen species in immortalized brain microglia (BV2): Implications for nanoparticle neurotoxicity. *Environ Sci Technol* 2006;40(14):4346-52.
21. Carmody RJ, Cotter TG. Signalling apoptosis: A radical approach. *Redox Rep* 2001;6(2):77-90.
22. Ryter SW, Kim HP, Hoetzel A, Park JW, Nakahira K, Wang X, *et al*. Mechanisms of cell death in oxidative stress. *Antioxid Redox Signal* 2007;9(1):49-89.